Interaction of Verapamil with Lipid Membranes and P-Glycoprotein: Connecting Thermodynamics and Membrane Structure with Functional Activity

M. Meier, X. Li Blatter, A. Seelig, and J. Seelig
Department of Biophysical Chemistry, Biozentrum, University of Basel, Basel, Switzerland

ABSTRACT Verapamil and amlodipine are calcium ion influx inhibitors of wide clinical use. They are partially charged at neutral pH and exhibit amphiphilic properties. The noncharged species can easily cross the lipid membrane. We have measured with solid-state NMR the structural changes induced by verapamil upon incorporation into phospholipid bilayers and have compared them with earlier data on amlodipine and nimodipine. Verapamil and amlodipine produce a rotation of the phosphocholine headgroup away from the membrane surface and a disordering of the fatty acid chains. We have determined the thermodynamics of verapamil partitioning into neutral and negatively charged membranes with isothermal titration calorimetry. Verapamil undergoes a pK-shift of $\Delta pK_a = 1.2$ units in neutral lipid membranes and the percentage of the noncharged species increases from 5% to 45%. Verapamil partitioning is increased for negatively charged membranes and the binding isotherms are strongly affected by the salt concentration. The electrostatic screening can be explained with the Gouy-Chapman theory. Using a functional phosphate assay we have measured the affinity of verapamil, amlodipine, and nimodipine for P-glycoprotein, and have calculated the free energy of drug binding from the aqueous phase to the active center of P-glycoprotein in the lipid phase. By combining the latter results with the lipid partitioning data it was possible, for the first time, to determine the true affinity of the three drugs for the P-glycoprotein active center if the reaction takes place exclusively in the lipid matrix.

INTRODUCTION

Broad-spectrum resistance to chemotherapeutic agents has been termed multidrug resistance (MDR). Although several mechanisms may contribute to MDR in mammalian cells, the best characterized is the efflux or flippase activity of the 170 kDa plasma membrane protein P-glycoprotein (Pgp, MDR1, or ABCB1). Pgp binds its substrates in the cytosolic leaflet of the lipid membrane and flips them to the extracellular leaflet or exports them to the extracellular environment (for review see (2)). Substrate binding to Pgp is best described by a two-step mechanism consisting of 1), a lipid-water partitioning step followed by 2), a binding to the transporter in the lipid phase (*l*) (3,4). The overall binding constant K_{tw} for the binding from the aqueous phase (*w*) to the transporter (*t*) can thus be expressed as product of the lipid-water partition coefficient, K_{lw}, and the transporter binding constant in the lipid phase, K_{tl} (5). We measured the transporter-water binding constant, K_{tw}, and the lipid-water partition coefficient, K_{lw}, for several structurally different drugs and derived the corresponding free energies of binding ΔG^0_{tw} and ΔG^0_{lw}. The free energy of substrate binding to Pgp in the lipid membrane, ΔG^0_{tl}, cannot be measured directly but was determined as the difference $\Delta G^0_{tl} = \Delta G^0_{tw} - \Delta G^0_{lw}$ (6). The value ΔG^0_{tl} can be rationalized with a modular binding concept based on hydrogen-bond formation (6–8).

The quantitative understanding of the two-step Pgp binding mechanism is of importance for efficient pharmacotherapy as well as for drug design. We therefore have selected three calcium channel blockers (verapamil, amlodipine, and nimodipine) of chemically different structure but similar numbers of hydrogen-bond modules (Fig. 1) for a detailed thermodynamic and functional study. Verapamil (pK_a 8.9 (9)) and amlodipine (pK_a 8.6 (10)) are positively charged at pH 7.4 whereas nimodipine is electrically neutral. Using thermodynamic and spectroscopic techniques we examine the partitioning of verapamil into phospholipid membranes and compare it to previous studies on amlodipine and nimodipine (11). The structure of the lipid membrane at different concentrations of verapamil was elucidated with solid-state NMR methods using selectively deuterated lipids. The influence of verapamil on the order of the lipid membrane is of special interest since it was claimed that a decrease in membrane order would reduce the activity of Pgp (for review, see (12,13)). The thermodynamic results are correlated with a functional assay for the binding of the three calcium-channel antagonists to Pgp in inside-out vesicles of MDR1-transfected mouse embryo fibroblasts (NIH-MDR1-G185) (14,15) and compared to extracellular acidification rate measurements performed with living cells (6,16,17).

MATERIALS AND METHODS

Materials

Verapamil hydrochloride was purchased from Fluka Biochemika (Buchs, Switzerland), amlodipine maleate from Sequoia Research Products (Pangbourne, United Kingdom), and nimodipine from Sigma-Aldrich (Sternheim, Germany). 1-palmitoyl-2-oleoyl-*sn*-glycero-3-phosphocholine

Submitted May 23, 2006, and accepted for publication July 17, 2006.

Address reprint requests to J. Seelig, Tel: 41-61-267 2190; E-mail: joachim.seelig@unibas.ch.

0006-3495/06/10/2943/13 $2.00

doi: 10.1529/biophysj.106.089581

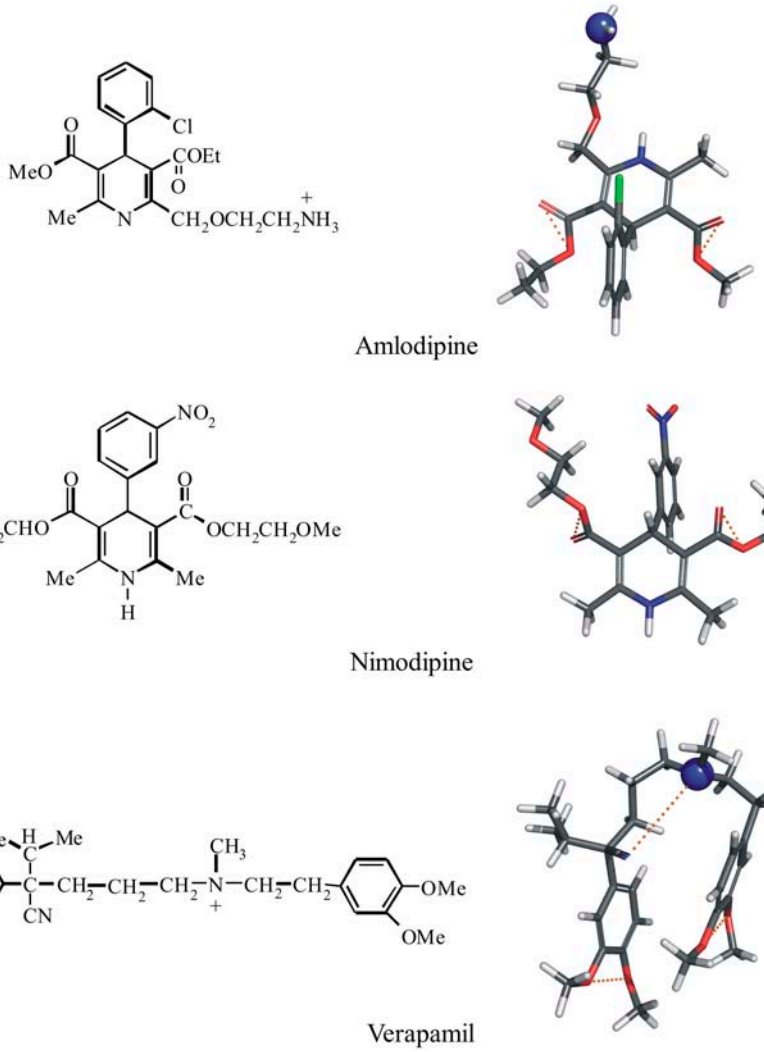

FIGURE 1 Chemical structures and conformational models of three calcium channel antagonists: verapamil, nimodipine, and amlodipine. The three-dimensional structures were obtained by searching the most amphiphilic, energy-minimized conformation with the minimal cross-sectional area, A_D. Oxygen and nitrogen molecules are shown in red and blue, respectively. Hydrogen-bond acceptors, constituting the binding modules for P-glycoprotein, are connected with dotted yellow lines. Pgp does not accept secondary amino groups (−NHR) or $-NO_2$ groups (for details, see (7)).

(POPC), 1,2-dioleoyl-trimethylammonium-propane (DOTAP), and 1-palmitoyl-2-oleoyl-*sn*-glycero-3-phosphoglycerol (POPG) were from Avanti Polar Lipids (Alabaster, AL). All other chemicals were purchased at highest purity from commercial sources.

Preparation of lipid vesicles

Small unilamellar vesicles (SUVs) of ~30 nm diameter were prepared as follows. Defined amounts of lipid were dissolved in chloroform and were dried first with a stream of N_2 and then overnight under high vacuum. For binary lipid mixtures the second lipid was added in chloroform solution to the dried film of the first lipid and treated as before. Subsequently, buffer solution (typically 50 mM HEPES, pH 7.4, plus various NaCl concentrations) was added to the lipid film and the mixture was vortexed extensively. Next, the lipid dispersion was sonicated under a nitrogen atmosphere for 10–25 min (at 10°C) until a clear solution was obtained. Metal debris from the titanium tip was removed by centrifugation at 14,000 *g* for 10 min.

Cell lines and cell culture

The mouse embryo fibroblast cell lines NIH3T3 and NIH3T3 transfected with the human *MDR1* gene, NIH-MDR-G185, were generously provided by Dr. M. M. Gottesman, National Institutes of Health, Bethesda, MD. Cells were maintained as described earlier (16,17). From these cells crude membranes were prepared as described elsewhere (17,18).

NMR measurements

POPC was deuterated either at the α- or β-position of the choline headgroup or at the *cis*-double bond of the oleic acyl chain (carbon atoms C-9′, C-10′) (19,20),

$$-\underset{\alpha}{POCH_2}\ \underset{\beta}{CH_2N}-$$

A defined amount of deuterated lipid was transferred into a NMR sample tube (typically 10–20 mg lipid) and drug/buffer solution was added to achieve a predefined drug/lipid ratio. For all NMR samples we used 25 mM MES, pH 5.5, and 100 mM NaCl as buffer. The concentration of verapamil was determined before mixing by UV spectroscopy at $\lambda = 277$ nm ($\varepsilon = 5818.8\ M^{-1}\ cm^{-1}$). To achieve a homogeneous suspension, the sample was extensively vortexed at room temperature with several freeze-thaw cycles in-between. Centrifugation at 30,000 *g* for 60 min at room temperature led to a clear supernatant. To calculate the molar amount of verapamil bound per mol of POPC, X_b (mol/mol), the verapamil concentration in the supernatant was determined again. A flat baseline above 380 nm was used as a criterion

for complete lipid removal. All ^{2}H-NMR experiments were performed on a Bruker Avance 400 MHz spectrometer (Bruker AXS, Berlin, Germany). ^{2}H-NMR spectra were recorded at 64 MHz with the quadrupole echo technique. The lipid pellets were used without further manipulations. ^{2}H-NMR spectra simulation was done with the NMR WebLab V.4.0 program (21). ^{31}P-NMR spectra were recorded at 161 MHz using a Hahn echo sequence with broadband proton decoupling (WALTZ-16) and a recycle delay of 6 s. The chemical shielding anisotropy, $\Delta\sigma$, was measured as full width at 10% maximum intensity.

Isothermal titration calorimetry

Isothermal titration calorimetry was performed with a VP ITC instrument (Microcal, Northampton, MA). Unless noted otherwise, measurements were made at 37°C. Appropriate buffer solutions were freshly prepared and the pH was properly adjusted when the temperature was changed. The sample cell contained the verapamil solution at a concentration of typically 100 μM. Lipid vesicles suspended in the same buffer as verapamil (lipid concentration of ~25–30 mM) were placed in a 300 μL syringe. Five microliter injections were made every 5 min. As a control, lipid vesicles were injected into the calorimeter cell containing buffer without verapamil.

Analysis of the ITC data

The classical way to describe drug partitioning into the lipid phase is to use the bulk concentration, $C_{D,eq}$. Here $C_{D,eq}$ is the equilibrium drug concentration far from the membrane surface. The amount of bound drug, $X_b = n_D/n_L^0$, is then given by

$$X_b = KC_{D,eq}. \quad (1)$$

Here n_D is the molar amount of bound drug and n_L^0 is the total lipid available for binding (for charged drugs that cannot permeate the lipid membrane, n_L^0 is the lipid on the outer vesicle surface). This simple partitioning law is valid for neutral drug molecules such as nimodipine. A more complex situation is encountered for charged drugs as the adsorption of the cationic amphiphiles leads to a positive surface potential ψ, repelling ions of like charge. Alternatively, the membrane may contain negatively charged lipids, producing a negative surface potential. Under these conditions, drug binding is increased because of electrostatic attraction. In both cases, the drug concentration at the plane of binding, $C_{D,M}$, is not identical to the bulk concentration, $C_{D,eq}$, but is given by

$$C_{D,M} = C_{D,eq}e^{-z_D\psi F_0/RT}, \quad (2)$$

where z_DF_0 is the molar electric charge, and RT is the thermal energy. The partition equilibrium Eq. 1 can then be modified as

$$X_b = K_pC_{D,M}. \quad (3)$$

Electrostatic attraction/repulsion effects are thus explicitly taken into account. Equation 3 predicts a linear relationship between the extent of membrane-bound drug and the drug surface concentration. Comparison with Eq. 1 demonstrates that K is not constant for charged drugs but depends on the surface potential and the effective charge according to $K = K_pe^{-zF_0\psi/RT}$. Consequently, K varies with the drug and salt concentration. For a monovalent drug such as verapamil and anionic POPC/POPG (75:25 mol/mol) membranes in 0.1 M NaCl, K is typically 5–10 times larger than K_p (verapamil concentration is in the mM-range). The surface potential, ψ, can be evaluated with the Gouy-Chapman theory (22,23) and the details of this analysis have been described previously (11,24). The analysis includes the binding of Na^+ ions to phosphatidylglycerol using the Langmuir adsorption isotherm with a Na^+ binding constant of 0.6 M^{-1}. In this evaluation the HEPES buffer was counted as a 1:1 salt. The sulfonic acid has a $pK_a \sim 3.6$ (25) and is fully charged; the counterion is Na^+. The piperazin ring is 50% charged. This latter effect was not included.

Surface activity measurements

Surface activity measurements were performed at ambient temperature and pH 7.4 (50 mM Tris buffer, 114 mM NaCl) (26,27). Due to the low solubility of amlodipine and nimodipine in water, stock solutions were prepared in methanol. The total concentration of methanol in the Langmuir trough was, however, <5% v/v. The surface activity was corrected for the effect of methanol. Despite this correction, the surface activity of charged drugs dissolved in methanol tends to be slightly higher than that of drugs dissolved in water due to a small pK_a shift. To obtain comparable experimental conditions, verapamil was also injected as methanolic stock solution, despite its better water solubility.

Pgp-ATPase activation assay

The P-glycoprotein associated ATPase activity was measured according to Litman et al. (15) in a 96-well microtiter plate. The ATPase assay buffer contained 25 mM Tris-HCl, 50 mM KCl, 3 mM ATP, 2.5 mM $MgSO_4$, 3 mM DTT, 0.5 mM EGTA, 2 mM ouabain, and 3 mM sodium azide, where the latter three compounds were used to inhibit the Ca-, the Na/K-, and the mitochondrial ATPase, respectively. The assay buffer was adjusted to pH 7.4 at 37°C. Membrane vesicles were diluted to a protein concentration of 0.1 mg/ml in ice-cold ATPase assay buffer. Each series of experiments contained 5 μg protein in a total assay volume of 60 μl. Incubation with the various drugs was started by transferring the plate from ice to a water bath, where it was kept 1 h at 37°C. The reaction was terminated by rapidly cooling the plate on ice. The released inorganic phosphate was determined by adding to each well an ice-cold stopping medium (200 μl) containing the color reagent (sulfuric acid 1.43% v/v; and SDS, 0.9% w/v), ammonium molybdate (0.2% (w/v)), and freshly prepared ascorbic acid (1% (w/v))). After incubation at room temperature for 30 min, the released phosphate was quantified calorimetrically at 820 nm using a microplate reader Spectramax M2 (Molecular Devices, Sunnyvale, CA). To determine the vanadate-sensitive Pgp ATPase activity, control samples were incubated in parallel with 500 μM vanadate and the values were subtracted from the values of the Pgp ATPase activation measurements. For stock solutions, drugs were dissolved in DMSO. The DMSO content of the sample was 1.67% (v/v). The data were analyzed according to the model proposed by Litman et al. (15),

$$V_{sw} = \frac{K_1K_2V_{bas} + K_2V_1C_{sw} + V_2C_{sw}^2}{K_1K_2 + K_2C_{sw} + C_{sw}^2}, \quad (4)$$

where V_{sw} is the rate of P_i release as a function of C_{sw}, the substrate concentration in aqueous solution; V_{bas} is the basal activity of Pgp in the absence of drug; V_1 is the maximum transporter activity (if only activation occurred); and V_2 is the minimum activity at infinite substrate concentration. At a substrate concentration, $C_{sw} = K_1$, half-maximum binding of the activating binding region is reached and at a substrate concentration, $C_{sw} = K_2$, half-maximum binding of the inhibitory binding region is reached.

RESULTS

Verapamil-induced structural changes of the lipid bilayer

Fig. 2 shows ^{2}H-NMR spectra obtained with coarse liposomes composed of POPC, deuterated at the α-segment of the choline moiety ($-POCD_2CH_2N-$) and measured in buffer at pH 5.5. Under these conditions, verapamil carries a charge of $z = +1$ (pK_a 8.9, at 25°C (9)).

All spectra are characteristic of liquid crystalline bilayers with a single quadrupole splitting seen at all drug concentrations. A single, time-averaged quadrupole splitting is also

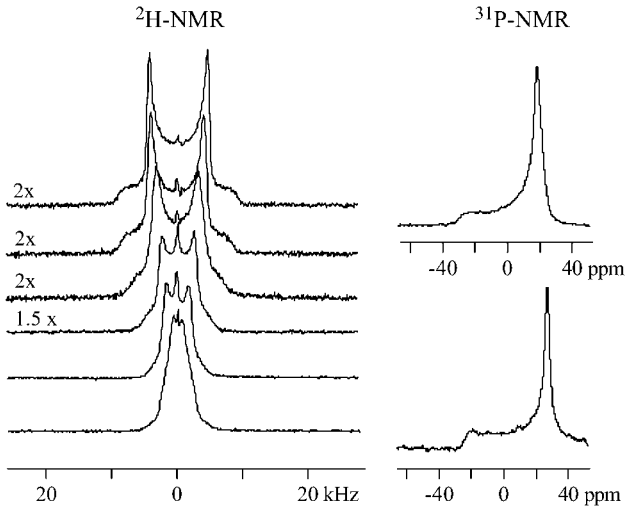

FIGURE 2 Deuterium and phosphorus-31 NMR spectra of POPC liposomes deuterated at the α-position of the choline headgroup ($-POCD_2CH_2N^+$). Approximately twenty-five milligrams of POPC was suspended in 50 μL buffer (25 mM, MES 0.1 M NaCl, pH 5.5, deuterium-depleted water) containing different concentrations of verapamil. The two top spectra correspond to pure POPC membranes without verapamil. The spectra below are characterized by increasing drug concentrations. The verapamil/POPC molar ratio from top to bottom is: 0, 0.02, 0.04, 0.07, 0.11, and 0.14. Virtually all verapamil is incorporated into the membrane. (Number of FIDs: ^{2}H NMR spectra 8 K, ^{31}P NMR 2 K.)

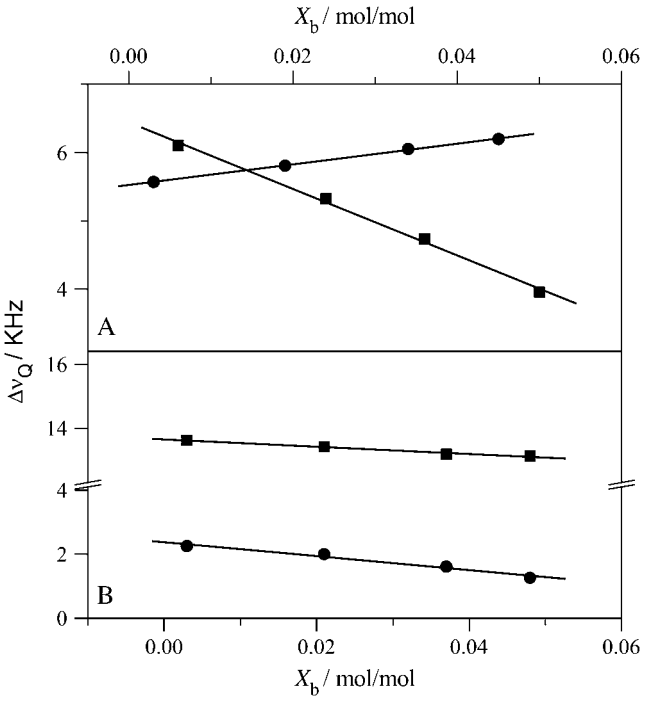

FIGURE 3 Variation of the deuterium NMR quadrupole splittings of POPC membranes with the verapamil/lipid molar ratio. (*A*) Phosphocholine headgroup segments: (■) α-CD_2 POPC ($-POCD_2CH_2N$); (●) β-CD_2-POPC ($-POCH_2CD_2N^+$). (*B*) POPC deuterated at the *cis*-double bond of the oleic acyl chain: (■) C-9′ deuteron, (●) C-10′ deuteron. Measurements at 22°C in buffer (MES 25 mM + 0.1 M NaCl, pH 5.5).

found for the β-segment of the choline headgroup and the *cis*-double bond of the oleic acyl chain (carbon atoms C-9′, C-10′). Apparently, the mobility of verapamil in the lipid membrane is fast enough so that the presence of the drug is sensed by all lipids in the bilayer within 10^{-5} s even at low drug concentration. The quadrupole splitting, $\Delta\nu_Q$, which is defined as the separation of the two most intense peaks in the deuterium NMR spectrum, is gradually changed as the molar verapamil/POPC ratio increases. The quadrupole splittings of the labeled carbon atoms are plotted in Fig. 3 as a function of bound drug, X_b (mol drug bound per mol lipid), revealing a linear relationship between the two parameters. For the two headgroup segments, linear regression analysis yields

$$\Delta\nu_Q(\alpha) = 6.45 - 46.14\,X_b(\text{kHz}) \quad (5)$$

and

$$\Delta\nu_Q(\beta) = 5.5 + 15.3\,X_b(\text{kHz}). \quad (6)$$

Fig. 2 also demonstrates that the quadrupole splitting of the α-segment collapses to a single line at a mole fraction of $\sim X_b \sim 0.14$. The bilayer structure remains, however, unchanged as evidenced by the phosphorus-31 NMR spectra shown next to the corresponding deuterium NMR spectra. The phosphorus-31 NMR spectra with and without verapamil are very similar and exhibit the typical signature of the bilayer phase (28). The chemical shielding anisotropy is $\Delta\sigma = -47.9$ ppm and remains approximately constant in the concentration range investigated. From the shape of the phosphorus-31 NMR spectra it can be concluded that the long-range structure of the bilayer remains unaltered. The deuterium NMR spectra, on the other hand, provide evidence for a change in the orientation of the choline dipole.

The verapamil-induced orientational change of the phosphocholine headgroup can be specified in more detail. Binding of the cationic verapamil to neutral POPC membranes imparts a positive electric charge onto the membrane surface. The orientation of choline headgroup P-N^+ vector with respect to the membrane surface is, however, dependent on the membrane surface charge density (29). In particular, a positive surface charge moves the N^+ end of the P-N^+ dipole toward the water phase. This change in orientation entails a counterdirectional response of the quadrupole splittings of the α- and β-segment such that $\Delta\nu_Q(\alpha)$ decreases and $\Delta\nu_Q(\beta)$ increases. Indeed, this counterdirectional change of the quadrupole splitting of the two choline segments is also observed for verapamil (Fig. 3). The extent of the out-of-plane rotation cannot yet be quantitated but exceeds that induced by amlodipine (11) or other monovalent hydrophobic drugs when applied at a similar membrane concentration (30).

The influence of verapamil on the hydrophobic part of the bilayer membrane was also examined with deuterium NMR. The deuterium labels were attached to the *cis*-double bond (C-9′ and C-10′ segment) of the *sn*-2 oleic acyl chain of POPC.

The two deuterons give rise to two separate quadrupole splittings with separations of 13.5 (C-9′) and 2.3 kHz (C-10′), even though they are connected to the same rigid structure (see Fig. 4). The molecular origin of this effect is a tilting of the *cis*-double bond with respect to the bilayer normal (20).

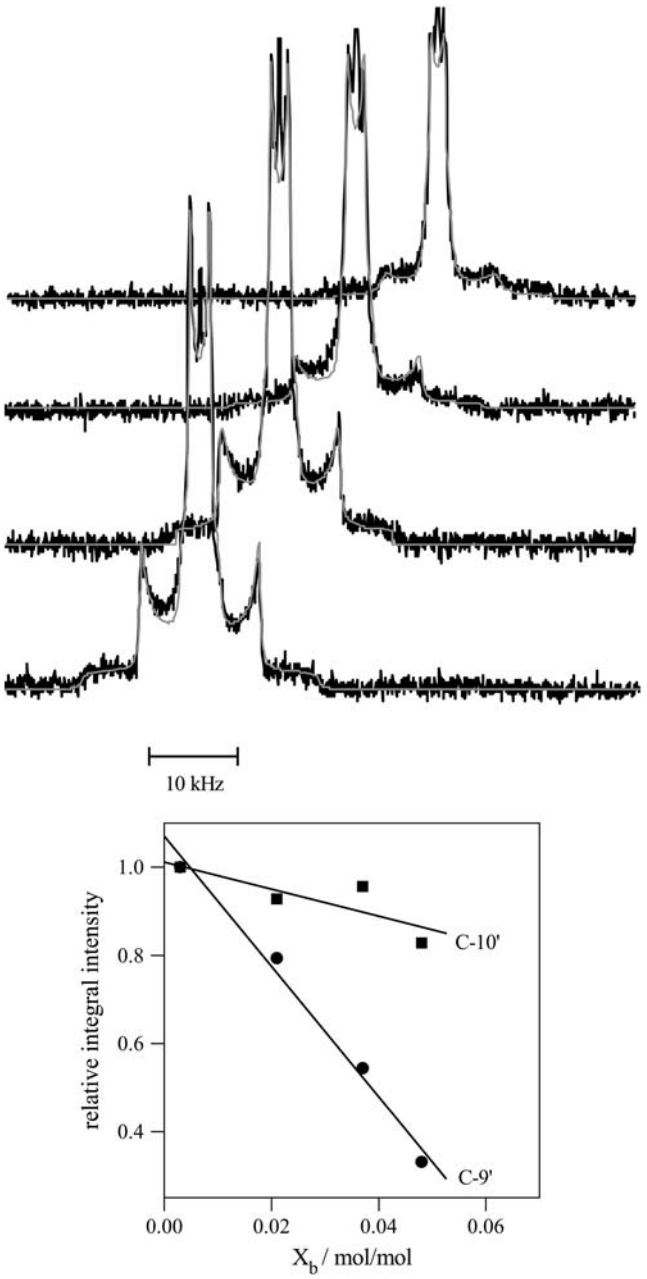

FIGURE 4 ^{2}H-NMR spectra of POPC membranes deuterated at the *cis*-double bond of the *sn*-2-oleic acyl chain and suspended in buffer with various verapamil concentrations. Approximately twenty-five milligrams of lipid suspended in 50 μL buffer (MES 25 mM + 0.1 M NaCl, pH 5.5) were used. The verapamil/lipid molar ratios from bottom-to-top are 0.003, 0.021, 0.037, and 0.048. The smooth lines are the simulated deuterium NMR spectra. The lower panel shows the loss in signal intensity of the C-9′ and C-10′ deuteron as a function of the verapamil/lipid molar ratio referenced to the pure POPC spectrum. The C-9′ deuteron with a 13 kHz splitting shows a much steeper intensity loss than the C-10′ deuteron with a 2 kHz splitting. (4 K free induction decays for all spectra.)

The variation of these quadrupole splittings with the mole fraction of bound verapamil is included in Fig. 3. The quadrupole splittings of both deuterons are moderately decreased upon increasing the verapamil concentration, according to

$$\Delta\nu_Q(\text{C-9}') = -11.5\,X_b + 13.65\,(\text{kHz}) \quad (7)$$

and

$$\Delta\nu_Q(\text{C-10}') = -21.9\,X_b + 2.3\,(\text{kHz}). \quad (8)$$

The fact that both quadrupole splittings decrease simultaneously suggests a disordering of the hydrophobic core upon verapamil intercalation, that is, a more random motion of the *cis*-double bond. This is quite different from amlodipine and nimodipine, which induce a small increase in the C-9′ and C-10′ quadrupole splittings (11).

Fig. 4 illustrates a second effect induced by the incorporation of verapamil into the lipid bilayer but limited to the hydrophobic region. All spectra in Fig. 4 were measured under identical conditions, in particular, the same number of free induction decays. Inspection of Fig. 4 nevertheless reveals a loss in signal intensity with increasing amount of verapamil in the membrane, which can be quantified by spectral simulation (*smooth lines* in Fig. 4). The spectrum with the lowest verapamil concentration serves as a reference spectrum and the areas under the two quadrupole splittings of this spectrum are identical (1:1 intensity ratio, Fig. 4, *lower panel*). At the highest verapamil concentration ($X_b = 0.43$) the intensity of the C-10′ deuteron is still 83% of the initial intensity; that of the C-9′ deuteron, however, is reduced to 33%. The most likely explanation of this effect is a reduction in the rate of motion of the *cis*-double bond caused by a weak complex formation with the aromatic ring system of verapamil. The reduced rate of motion makes the refocusing of the quadrupole echo more difficult, particularly for large quadrupole splittings. Similar effects have been observed for amlodipine in POPC membranes (11) and for reconstituted lipid-protein systems such as sarcoplasmic reticulum membranes, cytochrome c-oxidase, and rhodopsin (31–33). No intensity losses are observed for the α- and β-segments of the choline headgroup, indicating that the dynamics of the headgroup is not affected by the presence of verapamil.

Verapamil binding to lipid bilayers: variation of salt concentration and membrane charge

The adsorption of charged, amphipathic molecules to membranes involves electrostatic and hydrophobic interactions, protonation reactions, and dehydration effects. They contribute, to differing extent, to the heat measured in an isothermal titration calorimetry (ITC) experiment. As an example, Fig. 5 shows the titration of a 100 μM verapamil solution in buffer (50 mM HEPES, 50 mM NaCl, pH 7.4) with sonicated lipid

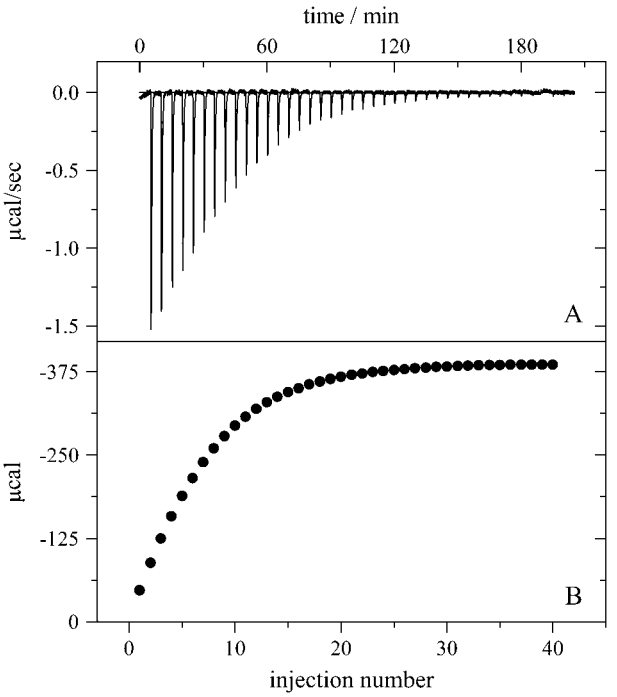

FIGURE 5 Titration of a 100 μM verapamil solution in 50 mM HEPES, pH 7.4 with 30 nm unilamellar lipid vesicles in the same buffer. Lipid composition is POPC/POPG (75:25 mol/mol). The injection of the lipid vesicles was in 5 μL steps. Measuring temperature 37°C. (*A*) Heat flow and (*B*) cumulative heat of reaction as a function of injection number.

vesicles composed of POPC/POPG (75/25 mol/mol). Verapamil is contained in the calorimeter cell ($V_{\text{cell}} = 1.4037$ mL) while the lipid suspension is injected at 5 μL aliquots. The total lipid concentration is 25 mM. Each lipid injection causes an exothermic binding reaction as revealed by the heat flow in Fig. 5 *A*. The size of the titration peak becomes smaller with increasing number of injections as less and less verapamil is available for binding. The integration of the heat flow peaks yield the heats of reaction, h_{i}, and Fig. 5 *B* displays the cumulative heat of reaction, Σh_{i}, as a function of the injection number *i*.

Fig. 5 further demonstrates that the reaction comes to completion after $n \sim 30$ injections. The molar binding enthalpy, ΔH_{D}^0, can then be calculated according to

$$\Delta H_{\text{D}}^0 = \sum_{\text{i}=1}^{\text{n}} h_{\text{i}}/n_{\text{D}}^0, \tag{9}$$

where n_{D}^0 is the total molar amount of verapamil in the calorimeter cell. Fig. 6 and Table 1 summarize the binding enthalpies, ΔH_{D}^0, of verapamil binding to POPC/POPG, POPC, and POPC/DOTAP membranes, as a function of total salt concentration (at 37°C). HEPES buffer was treated as a monovalent salt.

For negatively charged POPC/POPG vesicles the binding enthalpy is almost independent of the salt concentration and averages to $\Delta H_{\text{D}}^0 = -2.8 \pm 0.5$ kcal/mol. Neutral POPC and cationic POPC/DOTAP vesicles have ΔH_{D}^0 values in the

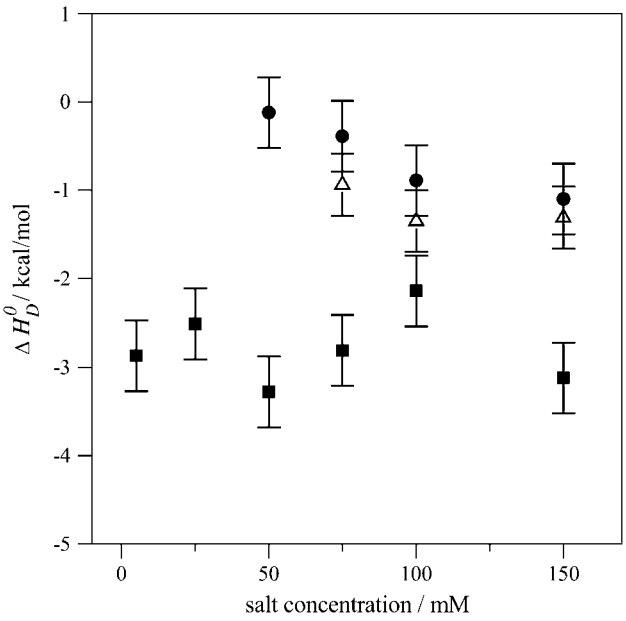

FIGURE 6 Reaction enthalpies of verapamil binding to phospholipid vesicles (30 nm) of different lipid composition. Variation of the binding enthalpy, ΔH_{D}^0, with the salt concentration. (■) POPC/POPG 75:25 mol/mol, (●) pure POPC, and (△) POPC/DOTAP 95:5 mol/mol.

range of -0.4 to -1.1 kcal/mol, which decrease with increasing salt concentration. At salt concentrations <50 mM for POPC and <75 mM for POPC/DOTAP (95:5 mol/mol), no heat of reaction could be observed. Also, no drug binding could be measured when the DOTAP molar percentage was raised above 10 mol %.

It is possible to deduce the amount of bound drug directly from the calorimetric titration according to

$$n_{\text{D,bound}}^{(\text{i})} = \sum_{\text{k}=1}^{\text{i}} h_{\text{k}}/(\Delta H_{\text{D}}^0 V_{\text{cell}} C_{\text{D}}^0), \tag{10}$$

where $n_{\text{D,bound}}^{(\text{i})}$ is the molar amount of bound drug after *i* injections, $\sum_{\text{k}=1}^{\text{i}} h_{\text{k}}$ is the cumulative heat of the first *i* injections, V_{cell} is the volume of drug solution in the calorimeter cell, and C_{D}^0 is the total drug concentration. The amount of free drug is then given from mass conservation as

$$n_{\text{D,free}}^{(\text{i})} = n_{\text{D}}^0 - n_{\text{D,bound}}^{(\text{i})}. \tag{11}$$

The degree of binding was defined above as

$$X_{\text{b}}^{(\text{i})} = n_{\text{D,bound}}^{(\text{i})}/\gamma n_{\text{L}}^0, \tag{12}$$

where n_{L}^0 is the total molar amount of lipid and γn_{L}^0 is the fraction of lipid accessible to the drug. It is hence possible to deduce the complete binding isotherm $X_{\text{b}} = f(c_{\text{eq}})$ from the calorimetric titration without invoking a specific binding model.

For POPC/POPG vesicles at pH 5.5, n_{L}^0 is only 60% of the total lipid ($\gamma = 0.6$), since the drug is fully charged and cannot translocate across the membrane. For all other measurements

TABLE 1 Thermodynamics of verapamil binding to phospholipids bilayer vesicles of different charge and size

SUV 30 nm	POPC mol %	POPG mol %	HEPES mM	NaCl	Drug electric charge near membrane surface $\langle z \rangle$	ΔH_D^0 kcal/mol	K_p M^{-1}	ΔG_D^0 kcal/mol
	75	25	50	100	0.84–0.89	−3.2	520	−3.84
	75	25	50	50	0.87–0.93	−2.1	400	−3.75
	75	25	50	25	0.88–0.94	−2.8	450	−3.75
	75	25	50	0	0.91–0.96	−3.3	300	−3.50
	80	20	25	0	0.91–0.97	−2.5	380	−3.65
	80	20	5	0	0.96–0.99	−2.9	330	−3.56
	100		50	100	0.57–0.63	−1.1	900	−4.18
	100		50	50	0.57–0.62	−0.9	800	−4.1
	100		50	25	0.53–0.61	−0.4	1200	−4.35
			TRIS					
	100		50	100	0.59–0.64	−3.1	900	−4.18
			PO_4^-					
	100		50	100	0.59–0.64	+1.4	750	−4.06
		DOTAP	HEPES					
	94.2	5.8	50	100	0.49–0.51	−1.1	500	−3.81
LUV								
100 nm	100		50	100	0.61–0.64	−1.0	470	−3.78
	100		50	50	0.61–0.63	−1.1	400	−3.68
	100		50	25	0.59–0.63	−0.6	500	−3.81

Note that all measurements are at 37°C, pH 7.4.

described in this study, a rapid translocation of verapamil across the membrane was assumed ($\gamma = 1$). For example, POPC/POPG vesicles at 150 mM salt and pH 7.4 exhibit a surface potential of ~−30 mV, which reduces the pH near the membrane surface to pH 6.8. At this pH, the neutral form of verapamil accounts for only 1% of the total drug concentration. However, upon entering the membrane, verapamil experiences a pK_a shift by 1.2 units (see below). Both effects together are sufficient to establish a rapid *trans*-membrane equilibrium.

Fig. 7 then displays ITC-derived binding isotherms for POPC/POPG bilayers at various salt concentrations. The strongest binding is observed for the lowest salt concentration where the electrostatic attraction between the anionic membrane and the cationic drug is maximal. All binding isotherms have a curved appearance and the binding constant defined according to Eq. 1 varies with the verapamil and salt concentration. At a verapamil concentration of $C_{D,eq} = 10$ μM, apparent binding constants are $K \sim 4 \times 10^3$ M^{-1}. In contrast, the solid lines in Fig. 7 were calculated with the Gouy-Chapman theory and a common binding constant $K_p = 410 \pm 30$ M^{-1} describes all three binding isotherms over the whole concentration range. The value K_p refers to the binding of the charged form of verapamil. Table 1 summarizes the K_p values for the different systems investigated. The value K_p is distinctly smaller than the apparent binding constant K, since the electrostatic attraction is not included.

For neutral POPC and cationic POPC/DOTAP vesicles at pH 7.4, the pH increases near the membrane surface and the fraction of the neutral form also increases. Membrane translocation of the drug is thus easily possible. Fig. 8 shows binding isotherms for POPC SUVs (three different salt concentrations) and for POPC/DOTAP SUVs. The extent of drug binding to POPC and POPC/DOTAP SUVs is clearly smaller than that observed for POPC/POPG SUVs at the same salt concentration. Electrostatic attraction/repulsion is the dominant factor for verapamil binding to charged membranes. For anionic POPC/POPG membranes the electrostatic

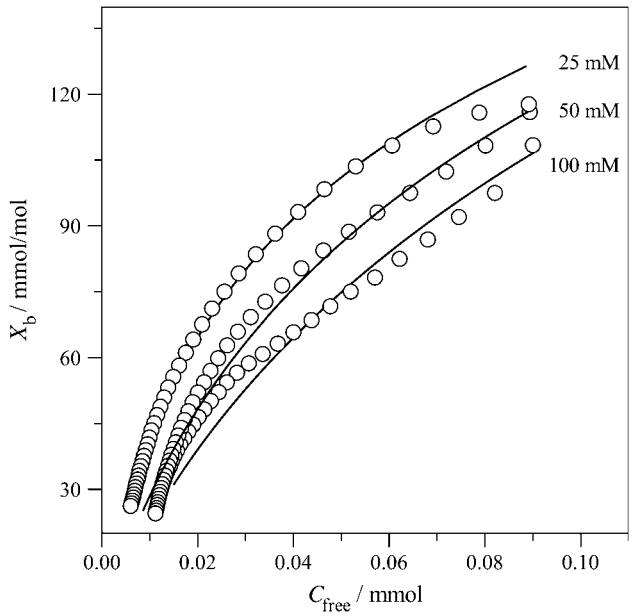

FIGURE 7 Verapamil binding isotherms for POPC/POPG membranes (75:25 mol/mol) at three different salt concentrations. All measurements made at pH 7.4 and 37°C. 50 mM HEPES + 50 mM NaCl; 50 mM HEPES; and 25 mM HEPES. The solid lines were calculated with the partition constants, K_p, given in Table 1 and the Gouy-Chapman theory. A rapid translocation of the neutral form of verapamil across the membrane was assumed.

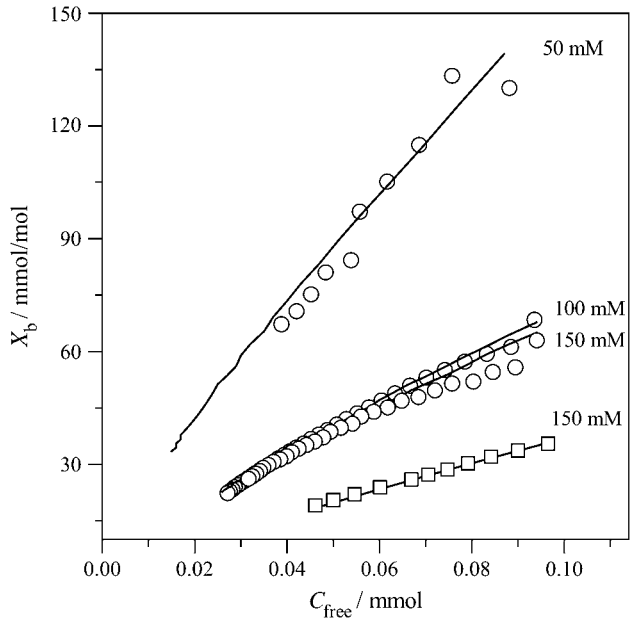

FIGURE 8 Binding of verapamil to POPC SUVs and mixed POPC/DOTAP (94.2:15.8 mol/mol) SUVs at various salt concentrations. (○) Pure POPC SUVs; (□) POPC/DOTAP SUVs. All measurements in 50 mM Tris or HEPES buffer + various concentrations of NaCl at 37°C: The solid lines are theoretical binding isotherms calculated with the partition coefficients listed in Table 1.

interaction is favorable, for cationic POPC/DOTAP membranes it is repulsive. However, even for neutral membranes, electrostatics is important since the membrane surface becomes positively charged as soon as the first cationic drug molecule is incorporated into the membrane. Further binding of drug molecules thus becomes increasingly more difficult. The solid lines in Fig. 8 were again calculated with the Gouy-Chapman theory.

The results described above were obtained with vesicles prepared by sonication, having an average diameter of ~30 nm (SUV). Verapamil binding to POPC membranes was also studied with unilamellar vesicles of 100 nm diameter (LUVs) prepared by extrusion through polycarbonate filters. LUVs exhibit a tighter lipid packing than SUVs and resemble more closely planar lipid bilayers. The ITC data were analyzed with the same model as described for SUVs. Again fast translocation of the drug (in its uncharged form) across the membrane was assumed. The experimental results are included in Table 1. The reaction enthalpy at 37°C is $\Delta H_D^0 = -1.1\,\text{kcal/mol}$ for SUVs and $\Delta H_D^0 \approx -1.0\,\text{kcal/mol}$ for LUVs. The binding constants, again deduced with the Gouy-Chapman theory, are somewhat smaller than those of SUVs (see Table 1).

Membrane-induced pK_a shift of verapamil

The ionization constant of verapamil in aqueous solution at 25°C is pK_a 8.9 (9). It is temperature-dependent and decreases with increasing temperature (see below). A decrease in pK_a can also be expected for verapamil entering the lipid membrane, because the neutral form is favored in the nonpolar environment. The pK_a shift was quantified by measuring the binding reaction in buffers of different dissociation enthalpies, since the reaction enthalpy is the sum of the verapamil deprotonation and the buffer protonation. Verapamil binding to POPC vesicles yields $\Delta H_D^0 = -3.0\,\text{kcal/mol}$ in 50 mM Tris buffer, $\Delta H_D^0 = -1.1\,\text{kcal/mol}$ in 50 mM HEPES buffer, and $\Delta H_D^0 = +1.4\,\text{kcal/mol}$ in phosphate buffer (all measurements at 100 mM NaCl, pH 7.4). This provides evidence for a deprotonation reaction (34–36) of verapamil as it enters the membrane. Fig. 9 shows a plot of the binding enthalpy, ΔH_D^0, versus the buffer dissociation enthalpy, ΔH_{buffer}, yielding

$$\Delta H_D^0 = -0.41\,\Delta H_{buffer} + 1.5. \quad (13)$$

From the slope it can be deduced that 0.41 H^+ dissociate upon verapamil insertion into the neutral POPC membrane. While the average charge of verapamil in solution at pH 7.4 is $\langle z_D \rangle = 0.97$ e.u., the membrane-bound drug carries an average charge of $\langle z_D \rangle \approx 0.56$ e.u. The reduction by $\delta z = 0.41$ e.u. can be traced back to two sources. Upon binding to the membrane, verapamil repels H^+ ions from the membrane surface. At 150 mM salt and 0.1 mM verapamil, the pH at the membrane surface increases to ~pH 7.6 and the electric charge of verapamil decreases concomitantly to $z = 0.95$ e.u. ($\delta z = 0.02$ e.u.). However, from the buffer dependence one deduces a much larger change of $\delta z = 0.41$ e.u., attesting to a

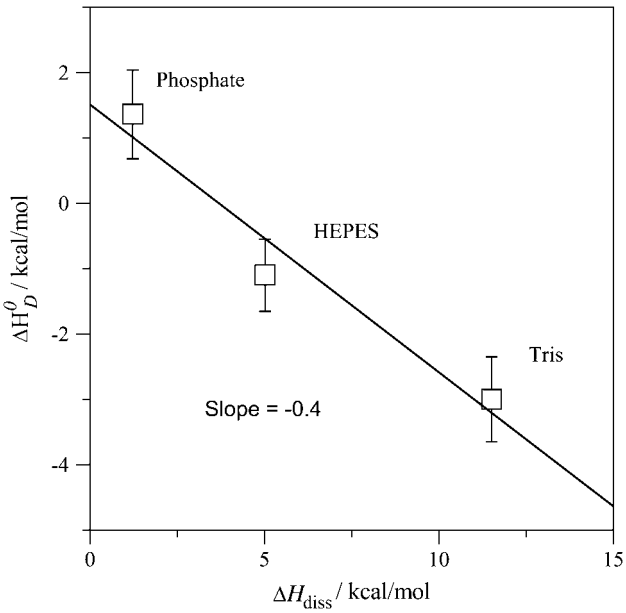

FIGURE 9 Variation of the verapamil binding enthalpies with the buffer dissociation enthalpies. POPC vesicles with 30 nm diameter. Measurements made in Tris ($\Delta H_{Diss} = 11.51$ kcal/mol), HEPES ($\Delta H_{Diss} = 4.9$ kcal/mol), and phosphate ($\Delta H_{Diss} = 1.22$ kcal/mol) at 37°C (36).

pK_a shift as the drug enters the hydrophobic environment. At pH 7.6, a pK_a shift from $pK_a \sim 8.9$ to $pK_a \sim 7.7$ reduces the charge from $\langle z \rangle = 0.95$ to $z = 0.56$ ($\delta z = 0.39$). The two effects together (pH change plus pK_a shift) then explain the experimental data. Based on chemical equilibria considerations it can be calculated that the uncharged drug has a $10^{\Delta pK_a} \sim 16$-times higher partition-coefficient for the lipid membrane than the protonated species. The binding constant of uncharged verapamil is thus $K_p = 6.5 \times 10^3\ M^{-1}$ for POPC/POPG membranes and $K_p \sim 1.6 \times 10^4\ M^{-1}$ for POPC vesicles (at pH 7.4 and 37°C).

For membranes composed of diphytanoyl PC, a dissociation constant for uncharged verapamil was estimated as $K_d = 0.061 \pm 0.01$ mM at pH 10.5 based on electrophoretic and membrane potential measurements (37). This translates into a binding constant of $K_p = 1.6 \times 10^4\ M^{-1}$.

We also measured the molar reaction enthalpy of verapamil binding to POPC vesicles at pH 5.5. At this pH, verapamil is fully charged and no deprotonation takes place upon binding to the membrane. The binding enthalpy was found to be $\Delta H_D^0(\text{pH}\,5.5) = -2.7\,\text{kcal/mol}$. On the other hand, the (extrapolated) binding enthalpy at pH 7.4 in the absence of a buffer dissociation reaction is ΔH_D (pH 7.4) = 1.5 kcal/mol (see Fig. 9 for $\Delta H_{Diss} = 0$). The value ΔH_D (pH 7.4) is thus composed of the binding enthalpy of the fully charged drug, ΔH_D (pH 5.5), plus the dissociation enthalpy for 0.41 H^+,

$$\Delta H_D(\text{pH}\,7.4) = \Delta H_D(\text{pH}\,5.5) + 0.41\Delta H_{Diss}^{NH}, \qquad (14)$$

where ΔH_{Diss}^{NH} is the dissociation enthalpy of the verapamil amino group. The latter is then calculated as $\Delta H_{Diss}^{NH} = 10.2\,\text{kcal/mol}$. This result is consistent with data obtained for N-terminal amino group of peptides where the dissociation energy is $\sim 11 \pm 2$ kcal/mol (38).

Heat capacity change ΔC_P^0

We have measured the temperature-dependence of the verapamil-membrane partition equilibrium. For PC/PG (75:25 mol/mol) membranes in 50 mM HEPES at pH 7.4, ΔH_D^0 shows only a small temperature-dependence with a molar heat capacity of $\Delta C_P^0 = 14\,\text{cal/mol K}$. For pure PC SUVs in buffer (100 mM NaCl, 50 mM HEPES, pH 7.4), the heat capacity change is $\Delta C_P^0 = 12\,\text{cal/mol K}$.

Molecular cross-sectional area and air-water partition coefficient

Amphiphilic molecules such as verapamil, amlodipine, and nimodipine partition into the air-water and lipid-water interface such that the polar groups remain in either the aqueous phase ($\varepsilon \approx 80$) or the polar headgroup region of the lipid membrane ($\varepsilon \approx 30$). The hydrophobic group is then exposed to air (dielectric constant, $\varepsilon \approx 1$) or inserts into the lipid core region ($\varepsilon \approx 2$). The approximate conformation of the three Ca^{2+} blockers, calculated by optimizing polar and nonpolar interactions, are shown in Fig. 1 (39). The cross-sectional areas of the three molecules, relevant for membrane insertion, were calculated as $A_D = 82$ Å^2 for verapamil, 66.2 Å^2 for amlodipine, and 69.4 Å^2 for nimodipine.

The surface activities of the three Ca^{2+} blockers were measured with the Wilhelmy plate method (data not shown) and were described by the Szyszkowski isotherm. The measured cross-sectional area of verapamil in aqueous solution is $A_D = 82 \pm 2$ Å^2 and in good agreement with the calculated value. The cross-sectional areas of amlodipine ($A_D = 122$ Å^2) and nimodipine ($A_D = 87$ Å^2) are, however, larger than the calculated data, which is caused by association effects at higher concentrations. For the following calculations, we use the calculated cross-sectional areas.

The air-water partition coefficients are $K_{A/W} = 1.7 \times 10^5\ M^{-1}$ for verapamil, $K_{A/W} = 1.9 \times 10^6\ M^{-1}$ for amlodipine, and $K_{A/W} = 7.1 \times 10^5\ M^{-1}$ for nimodipine. Insertion into the lipid bilayer expands the surface area and requires additional expansion work πA_D (40) where π is the monolayer-bilayer equivalence pressure (41). The lipid-water partition coefficient can then be calculated from the air-water partition coefficient as $K_{Lip/W} = K_{A/W} \exp(-\pi A_D/kT)$ (26). For POPC LUVs (100 nm) and planar membranes with an equivalence pressure of $\pi \sim 30$ mN/m, the lipid-water partition coefficient of charged verapamil is predicted to be $K_{lip/W} \approx 540\ M^{-1}$ in excellent agreement with the ITC measurements. For amlodipine $K_{lip/W} = 1.8 \times 10^4\ M^{-1}$, again in good agreement with previous ITC measurements ($K_p = 1.6 \times 10^4\ M^{-1}$ at pH 7.2, (11)). For nimodipine, the lipid water partition coefficient was calculated as $K_{lip/W} = 5.4 \times 10^3\ M^{-1}$. This value must be considered as a lower limit as nimodipine has a strong tendency to adsorb to the vessel walls. The data are summarized in Table 2.

P-glycoprotein transporter activity measurements with verapamil, amlodipine, and nimodipine

The P-glycoprotein transporter (Pgp) accepts its substrates from the cytosolic membrane leaflet. The Pgp transport efficiency is determined by 1), the lipid solubility of the substrate; and 2), the affinity of the substrate for the transporter in the lipid phase. The latter can be estimated on the basis of characteristic hydrogen-bonding patterns (6,7). Pgp shows basal activity in the absence of substrates. In the presence of substrates it follows a bell-shaped curve with an initial increase in activation (characterized by the concentration of half-maximum activation, K_1) followed by a decrease in activation at higher drug concentrations (characterized by the concentration of half-maximum inhibition, K_2). The model is detailed in references (6,15). Experimental results obtained with inside-out vesicles using a phosphate assay are shown in Fig. 10 for both verapamil and amlodipine. The quantitative analysis in terms of the model described by Litman

TABLE 2 Comparison of verapamil, amlodipine, and nimodipine; bilayer structure, binding thermodynamics, and P-glycoprotein activity

	Nimodipine	Amlodipine	Verapamil
Deuterium NMR			
Headgroup segments			
m_α (kHz/mol)	no effect*	−30.50*	−46.14
m_β (kHz/mol)	no effect*	15.25*	15.30
cis-double bond			
$m_{C\text{-}9'}$ (kHz/mol)			−11.50
$m_{C\text{-}10'}$ (kHz/mol)			−21.90
Surface activity measurements			
Cross-sectional area			
A_D (Å^2)	69.4	66.2	82
$K_{A/W}$ (M^{-1})†	7.1×10^{5}‡	1.9×10^{6}	1.7×10^{5}
$K_{lip/w}$ (M^{-1}) at 30 mN/m	5.4×10^{3}‡	1.8×10^{4}	540
ITC measurements			
K_p (M^{-1}) LUVS	nd	7.6×10^{3}§	470¶
ΔG^0_{tw}(kcal/mol)	−5.275	−5.484	−3.776
ΔH^0 (kcal/mol)	nd	−8.90§	−1.0¶
Max. electric charge	0	1	1
pK	—	8.6	8.9
Pgp activity			
K_1 (M)	7.9×10^{-7}	1.1×10^{-7}	9.5×10^{-7}
ΔG^0_{tw}(kcal/mol)	−8.624	−9.834	−8.511
K_2 (M)	—	3.9×10^{-5}	3.7×10^{-5}
V_1 (%)	2.06	2.13	2.6
Drug affinity in lipid bilayer			
ΔG^0_{tl}(kcal/mol)	−3.35	−4.350	−4.735
K_{tl} (M^{-1})	234	1200	2240
No. of H-bond acceptors	4	4	5
ΔG^0_{Hi}(J/mol)	−0.84	−1.088	−0.947

*Data taken from Bäuerle et al. (11).
†Data obtained with methanolic stock solutions (see Materials and Methods).
‡Lower limit due to adsorption to the Teflon trough.
§Multilamellar POPC liposomes, 0.1 M NaCl, 10 mM Tris, pH 7.25. Bäuerle et al. (11) gives $K_p = 1.55 \times 10^4$ M^{-1} and $\Delta H^0 = -8.9$ kcal/mol at 23°C. Using van′ t Hoff's law and assuming a temperature-independent ΔH^0, K_p was recalculated for 37°C.
¶100 nm POPC LUVs, 0.1 M NaCl, 50 mM HEPES, pH 7.4, 37°C.

et al. (15) yields the parameters K_1, K_2 and also the corresponding reaction velocities V_1 and V_2. The data are summarized in Table 2. As outlined previously, the parameters K_1 and K_2 can be interpreted as dissociation constants. Table 2 reveals that amlodipine has a higher affinity to Pgp than verapamil during the activation phase. Whereas the inhibition phase can be well measured for verapamil it cannot be measured to high concentrations for amlodipine and nimodipine due to drug association in solution. Partitioning into the lipid membrane requires the monomeric form of drugs and is not possible at concentrations which are higher than the critical micelles concentration.

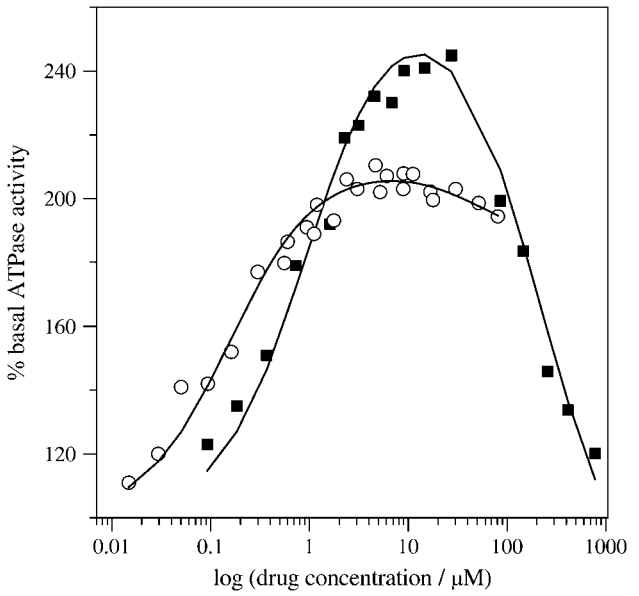

FIGURE 10 Pgp activation profiles obtained by a phosphate release assay with inside-out vesicles prepared from NIH-MDR-G185 cells. (■) Verapamil; (○) amlodipine.

DISCUSSION

Structural aspects of verapamil binding

Verapamil HCl is a calcium-ion influx inhibitor of wide clinical use. It is administered as a racemic mixture of R- and S-enantiomers. At low drug concentration and pH 7.4, a neutral (3%) and a charged species (97%) are in equilibrium in aqueous solution. The molecule exhibits amphiphilic properties and is well soluble in water, organic solvents, and lipid membranes. The pK_a-value of verapamil decreases distinctly with increasing temperature as the present ITC data show that the dissociation enthalpy is endothermic with $\Delta H^{NH}_{Diss} \sim 10$ kcal/mol.

Fig. 1 displays the conformations of verapamil, amlodipine, and nimodipine in the lipid membrane obtained by an energy minimization calculation (39). Verapamil adopts a folded conformation such that both aromatic ring systems can be inserted into the hydrophobic core of the membrane whereas the charged amino group remains at the lipid-water interface. Partitioning of verapamil into the lipid membrane modulates the lipid bilayer structure, as evidenced by deuterium NMR. The predominant effect in the hydrocarbon region is a disordering of the hydrocarbon chains and a weak complex formation of the *cis*-double bond with the aromatic rings of verapamil. Hydrocarbon chain disordering is a common phenomenon when proteins or other nonlipid components are inserted into the lipid bilayer (11,32). Particularly effective are detergent molecules (42,43), whereas cholesterol has the opposite effect; that is, the rodlike molecule induces a stiffening of the hydrocarbon chain (44–47). Membrane disordering has been implied in Pgp inactivation

but cannot play an important role for verapamil as this molecule is considered as the substrate per-excellence for specific drug-Pgp interactions. At the headgroup level, verapamil moves the $^{+}$N end of the choline dipole toward the water phase. Verapamil is more efficient than amlodipine in turning the $^{-}$P-N^{+} dipole since the change of the $\Delta\nu_Q(\alpha)$ quadrupole-splitting-per-mole-incorporated drug is $m_\alpha = -46.1$ kHz/mol for verapamil and only $m_\alpha = -30.5$ for amlodipine. Nimodipine as a noncharged molecule has no effect (11). The consequence of this change in dipole orientation is a change in the electric field across the bilayer membrane. The $^{-}$P-N^{+} dipole has a large dipole moment of ~25 Debye (48). If the $^{-}$P-N^{+} dipole is approximately parallel to the membrane surface, as in a pure POPC bilayer (49), the electric dipole field cannot penetrate deeply into the membrane. An orientation 20° away from the membrane surface can, however, creates a field of ~100 mV in the adjacent hydrophobic part of the membrane with its low dielectric constant of $\varepsilon = 2$. Dipole fields are not efficiently screened by salt and are thus long-range. The electric effect of a single verapamil molecule will therefore extend over several layers of surrounding phospholipids. Electric fields of 100 mV across a distance of 2 nm thickness correspond to a field strength of 5×10^7 V/m and can induce conformational changes in proteins.

Thermodynamic binding parameters and Pgp activation

The extent of partitioning of verapamil into a lipid bilayer membrane is influenced by the electric charge of the membrane surface and the screening of Coulombic interactions through inert electrolytes. This is illustrated with the binding isotherms obtained for negatively charged (Fig. 7) and neutral (Fig. 8) membranes. In both cases, increasing NaCl concentrations decrease the amount of bound verapamil. Negatively charged POPC/POPG (75/25 mol/mol) membranes exhibit a surface potential of −40 mV in 150 mM NaCl, decreasing to −115 mV in 5 mM NaCl. The verapamil binding-affinity increases in parallel with the electrostatic attraction (Fig. 7). By using surface concentrations, $C_{D,M}$, instead of bulk concentrations, the variation of electrostatic attraction can be accounted for, leading to constant intrinsic binding constant. The solid lines in Fig. 7 were simulated with similar binding constants ($K_p = 410 \pm 30$ M^{-1}; see Table 1). The average electric charge of verapamil is $\langle z \rangle \sim 0.85$–$0.99$.

A different situation is encountered for pure POPC bilayers. They are noncharged in the absence of verapamil and become positively charged upon drug binding. Under the present experimental conditions the surface potentials are small ($\psi \sim 5$–15 mV) and the binding constants determined with and without electrostatic correction differ by ~0–20% only. The insertion into the hydrophobic membrane entails a distinct pK$_a$-shift and the electric charge of verapamil in the membrane is only $\langle z \rangle \sim 0.5$. The binding constant of the charged species is $K_p \sim 400$–500 M^{-1} for LUVs but $K_p \sim 900$–1200 for SUVs. Verapamil binding to phosphatidylcholine bilayers was determined previously by a centrifugation assay at 22°C (1). For multilamellar liposomes composed of egg lecithin (which typically contains 40% POPC), a verapamil partition coefficient of $P_{Lipid} \sim 267$ was determined (see also Fig. 4).

Verapamil binding to POPC LUVs can be compared to related data obtained for amlodipine and nimodipine leading to the following order of partition coefficients K_p, for POPC LUVs (at 37°C): verapamil 470 M^{-1} < nimodipine ~ 5.4×10^3 M^{-1} < amlodipine 7.6×10^3 M^{-1} (see Table 2).

Lipid solubility is a prerequisite for a drug to be recognized by Pgp, since the active center of this enzyme is located in the inner part of the lipid membrane. The Pgp activity can be measured with a phosphate release assay or, alternatively, a Cytosensor assay (6). Both assays refer to the overall process, that is, the binding of the drug from the aqueous phase to the active center of the transporter in the lipid phase. The corresponding free energy, ΔG^0_{tw}, is given by $\Delta G^0_{tw} = RT \ln(K_1)$, where K_1 has been defined above as the dissociation constant derived from the activation part of the bell-shaped curve given by Eq. 4. The value ΔG^0_{tw} can be divided into two physically distinct processes, namely 1), the partitioning of the drug from water into the lipid membrane, ΔG^0_{lw}, followed by 2), the binding of the drug to the transporter in the lipid matrix, ΔG^0_{tl} (6):

$$\Delta G^0_{tw} = \Delta G^0_{lw} + \Delta G^0_{tl}. \quad (15)$$

ΔG^0_{lw} is related to the lipid-water partition coefficient according to $\Delta G^0_{lw} = -RT \ln K_p$. In this and previous studies we have measured K_p by ITC and by surface activity measurements. We thus know ΔG^0_{lw} for all three drugs from physical-chemical experiments. On the other hand, Pgp activation has been measured in the present study for verapamil, amlodipine, and nimodipine with the phosphate release assay leading to the overall free energy ΔG^0_{tw} (Table 2). Knowledge of ΔG^0_{tw} and ΔG^0_{lw} then allows the evaluation of ΔG^0_{tl}, i.e., the affinity of the drug for the transporter in the lipid phase. The corresponding results for verapamil, amlodipine, and nimodipine are $\Delta G^0_{tl} = -4.7$, -4.4, and -3.4 kcal/mol, respectively.

ΔG^0_{tl} can be further converted to lipid binding constants and it is thus possible, for the first time, to derive the binding constants of verapamil and amlodipine to Pgp in the lipid phase. The corresponding numbers are $K_{tl} = 2.24 \times 10^3$ for verapamil, 1.2×10^3 for amlodipine, and 230 for nimodipine.

We have previously proposed a model which explains the substrate versatility of Pgp on the basis of a modular binding concept, that is, Pgp recognizes well-defined hydrogen-bond acceptor groups (7). Not all hydrogen-bond acceptor groups form hydrogen bonds with same free energy. We distinguish among strong (oxygen atoms), intermediate (nitrogen and sulfur atoms, phenyl groups), and weak (fluorine atoms) hydrogen-bond acceptors, weighted with hydrogen-bond energy units of $EU_H = 1$, 0.5, and 0.25, respectively. This

model leads to $EU_H = 5$ for verapamil and $EU_H = 4$ for amlodipine and nimodipine, respectively. Based on the above free energy of binding in the lipid phase, ΔG^0_{tl}, the average bonding free energy per hydrogen bond is thus $\Delta G^0_{Hi} = -0.95\,\text{kcal/mol}(-1.1\,\text{kcal/mol}, -0.85\,\text{kcal/mol})$ for verapamil (amlodipine, nimodipine). This is in good agreement with a larger set of 15 drug molecules where the free energy of binding from water to the transporter was derived from Cytosensor measurements monitoring the extracellular acidification rate (see (6), Table 1). The average free energy per hydrogen bond was found to be $\Delta G^0_{Hi} \approx -0.79\,\text{kcal/mol}$.

Transport of calcium channel antagonists by Pgp

As Pgp accepts its substrates from the cytosolic leaflet, lipid solubility is an important prerequisite for a substrate to be recognized by Pgp. The second factor is the binding affinity of the drug to Pgp determined by the respective hydrogen-bonding patterns. The above analysis shows that verapamil exhibits the lowest lipid solubility but has the highest binding affinity to the transporter. If dissolved at equal concentrations in the lipid phase, verapamil is binding more efficiently than amlodipine or nimodipine. However, if dissolved at equal concentrations in the aqueous phase, amlodipine and nimodipine are more efficient in saturating Pgp because of their better lipid solubility. On the other hand, amlodipine and nimodipine diffuse more rapidly across the lipid membrane than verapamil due to the smaller cross-sectional area of the former two. Thus they can escape transport by Pgp more easily. Nimodipine, moreover, lacks the cationic charge and is thus not retained at the inner negatively charged membrane leaflet from which Pgp takes its substrates. Nimodipine can therefore be expected to cross the blood-brain barrier more easily. Indeed, in animal experiments, nimodipine had a strong effect on dilating the cerebral arteries, whereas the other two agonists act mainly on peripheral and cardiac vessels.

In conclusion, we have provided a complete binding analysis of verapamil and amlodipine to P-glycoprotein. We have dissected drug binding into a partitioning step into the lipid membrane, followed by the actual binding to the Pgp active site in the hydrophobic membrane. We could thus deduce the intrinsic binding constants of verapamil and amlodipine to Pgp in the lipid phase. All three drugs produce some disordering of the hydrocarbon chains. However, Pgp is not deactivated by membrane disordering as proposed previously.

G. Gerebtzoff was helpful in providing the computer figures and his scientific support is gratefully acknowledged.

This work was supported by the Swiss National Science Foundation grant No. 3100-107793.

REFERENCES

1. Romsicki, Y., and F. J. Sharom. 1999. The membrane lipid environment modulates drug interactions with the P-glycoprotein multidrug transporter. *Biochemistry*. 38:6887–6896.
2. Higgins, C. F., and M. M. Gottesman. 1992. Is the multidrug transporter a flippase? *Trends Biochem. Sci.* 17:18–21.
3. Lu, P., R. Liu, and F. J. Sharom. 2001. Drug transport by reconstituted P-glycoprotein in proteoliposomes. Effect of substrates and modulators, and dependence on bilayer phase state. *Eur. J. Biochem.* 268:1687–1697.
4. Omote, H., and M. K. Al-Shawi. 2006. Interaction of transported drugs with the lipid bilayer and P-glycoprotein through a solvation exchange mechanism. *Biophys. J.* 90:4046–4059.
5. Seelig, A., and E. Gatlik-Landwojtowicz. 2005. Inhibitors of multidrug efflux transporters: their membrane and protein interactions. *Mini Rev. Med. Chem.* 5:135–151.
6. Gatlik-Landwojtowicz, E., P. Aanismaa, and A. Seelig. 2006. Quantification and characterization of P-glycoprotein-substrate interactions. *Biochemistry*. 45:3020–3032.
7. Seelig, A. 1998. A general pattern for substrate recognition by P-glycoprotein. *Eur. J. Biochem.* 251:252–261.
8. Sauna, Z. E., M. B. Andrus, T. M. Turner, and S. V. Ambudkar. 2004. Biochemical basis of polyvalency as a strategy for enhancing the efficacy of P-glycoprotein (ABCB1) modulators: stipiamide homodimers separated with defined-length spacers reverse drug efflux with greater efficacy. *Biochemistry*. 43:2262–2271.
9. Hasegawa, J., T. Fujita, Y. Hayashi, K. Iwamoto, and J. Watanabe. 1984. pKa determination of verapamil by liquid-liquid partition. *J. Pharm. Sci.* 73:442–445.
10. Kass, R. S., J. P. Arena, and S. Chin. 1989. Cellular electrophysiology of amlodipine: probing the cardiac L-type calcium channel. *Am. J. Cardiol.* 64:35I–41I (discussion 41I–42I).
11. Bäuerle, H. D., and J. Seelig. 1991. Interaction of charged and uncharged calcium channel antagonists with phospholipid membranes. Binding equilibrium, binding enthalpy, and membrane location. *Biochemistry*. 30:7203–7211.
12. Eytan, G. D., R. Regev, G. Oren, and Y. G. Assaraf. 1996. The role of passive transbilayer drug movement in multidrug resistance and its modulation. *J. Biol. Chem.* 271:12897–12902.
13. Ferte, J. 2000. Analysis of the tangled relationships between P-glycoprotein-mediated multidrug resistance and the lipid phase of the cell membrane. *Eur. J. Biochem.* 267:277–294.
14. Al-Shawi, M. K., M. K. Polar, H. Omote, and R. A. Figler. 2003. Transition state analysis of the coupling of drug transport to ATP hydrolysis by P-glycoprotein. *J. Biol. Chem.* 278:52629–52640.
15. Litman, T., T. Zeuthen, T. Skovsgaard, and W. D. Stein. 1997. Structure-activity relationships of P-glycoprotein interacting drugs: kinetic characterization of their effects on ATPase activity. *Biochim. Biophys. Acta.* 1361:159–168.
16. Landwojtowicz, E., P. Nervi, and A. Seelig. 2002. Real-time monitoring of P-glycoprotein activation in living cells. *Biochemistry*. 41:8050–8057.
17. Gatlik-Landwojtowicz, E., P. Aanismaa, and A. Seelig. 2004. The rate of P-glycoprotein activation depends on the metabolic state of the cell. *Biochemistry*. 43:14840–14851.
18. Ambudkar, S. V. 1998. Drug-stimulatable ATPase activity in crude membranes of human MDR1-transfected mammalian cells. *Methods Enzymol.* 292:504–514.
19. Gally, H. U., W. Niederberger, and J. Seelig. 1975. Conformation and motion of the choline headgroup in bilayers of dipalmitoyl-3-*sn*-phosphatidylcholine. *Biochemistry*. 14:3647–3652.
20. Seelig, J., and N. Waespe-Sarcevic. 1978. Molecular order in *cis* and *trans* unsaturated phospholipid bilayers. *Biochemistry*. 17:3310–3315.
21. Macho, V., L. Brombacher, and H. W. Spiess. 2001. The NMR-WEBLAB: an internet approach to NMR lineshape analysis. *Appl. Magn. Reson.* 20:405–432.
22. Aveyard, R., and D. A. Haydon. 1973. Cambridge Chemistry Tests: An Introduction to the Principles of Surface Chemistry. Cambridge University Press, New York.
23. McLaughlin, S. 1977. Electrostatic potentials at membrane-solution interfaces. *Curr. Top. Membr. Transp.* 9:71–144.

24. Seelig, J., S. Nebel, P. Ganz, and C. Bruns. 1993. Electrostatic and nonpolar peptide-membrane interactions. Lipid binding and functional properties of somatostatin analogues of charge $z = +1$ to $z = +3$. *Biochemistry.* 32:9714–9721.

25. Goldberg, R. N., N. Kishore, and R. M. Lennen. 2002. Thermodynamic quantities for the ionization reactions of buffers. *J. Phys. Chem. Ref. Data.* 31:231–370.

26. Fischer, H., R. Gottschlich, and A. Seelig. 1998. Blood-brain barrier permeation: molecular parameters governing passive diffusion. *J. Membr. Biol.* 165:201–211.

27. Gerebtzoff, G., X. Li-Blatter, H. Fischer, A. Frentzel, and A. Seelig. 2004. Halogenation of drugs enhances membrane binding and permeation. *ChemBioChem.* 5:676–684.

28. Seelig, J. 1978. 31P nuclear magnetic resonance and the headgroup structure of phospholipids in membranes. *Biochim. Biophys. Acta.* 515:105–140.

29. Seelig, J., P. M. Macdonald, and P. G. Scherer. 1987. Phospholipid headgroups as sensors of electric charge in membranes. *Biochemistry.* 26:7535–7541.

30. Seelig, A., and J. Seelig. 2002. Membrane structure. *In* Encyclopedia of Physical Science and Technology, 3rd Ed. Academic Press, New York.

31. Seelig, J., L. Tamm, L. Hymel, and S. Fleischer. 1981. Deuterium and phosphorus nuclear magnetic resonance and fluorescence depolarization studies of functional reconstituted sarcoplasmic reticulum membrane vesicles. *Biochemistry.* 20:3922–3932.

32. Tamm, L. K., and J. Seelig. 1983. Lipid solvation of cytochrome c oxidase. Deuterium, nitrogen-14, and phosphorus-31 nuclear magnetic resonance studies on the phosphocholine headgroup and on *cis*-unsaturated fatty acyl chains. *Biochemistry.* 22:1474–1483.

33. Bienvenue, A., M. Bloom, J. H. Davis, and P. F. Devaux. 1982. Evidence for protein-associated lipids from deuterium nuclear magnetic resonance studies of rhodopsin-dimyristoylphosphatidylcholine recombinants. *J. Biol. Chem.* 257:3032–3038.

34. Flogel, M., and R. L. Biltonen. 1975. The pH dependence of the thermodynamics of the interaction of 3′-cytidine monophosphate with ribonuclease A. *Biochemistry.* 14:2610–2615.

35. Biltonen, R. L., and N. Langerman. 1979. Microcalorimetry for biological chemistry: experimental design, data analysis, and interpretation. *Methods Enzymol.* 61:287–318.

36. Morin, P. E., and E. Freire. 1991. Direct calorimetric analysis of the enzymatic activity of yeast cytochrome c oxidase. *Biochemistry.* 30:8494–8500.

37. Pohl, E. E., A. V. Krylov, M. Block, and P. Pohl. 1998. Changes of the membrane potential profile induced by verapamil and propranolol. *Biochim. Biophys. Acta.* 1373:170–178.

38. Martin, B. R. 1964. Introduction to Biophysical Chemistry. McGraw-Hill, New York.

39. Gerebtzoff, G., and A. Seelig. 2006. In-silico prediction of blood-brain barrier permeation using the calculated molecular cross-sectional area as main parameter. *J. Chem. Inf. Model.* In press.

40. Boguslavsky, V., M. Rebecchi, A. J. Morris, D. Y. Jhon, S. G. Rhee, and S. McLaughlin. 1994. Effect of monolayer surface pressure on the activities of phosphoinositide-specific phospholipase C-β 1, -γ1, and -δ1. *Biochemistry.* 33:3032–3037.

41. Seelig, A. 1987. Local anesthetics and pressure: a comparison of dibucaine binding to lipid monolayers and bilayers. *Biochim. Biophys. Acta.* 899:196–204.

42. Heerklotz, H., T. Wieprecht, and J. Seelig. 2004. Membrane perturbation by the lipopeptide surfactin and detergents as studied by deuterium NMR. *J. Phys. Chem. B.* 108:4909–4915.

43. Wenk, M. R., and J. Seelig. 1997. Interaction of octyl-β-thioglucopyranoside with lipid membranes. *Biophys. J.* 73:2565–2574.

44. Blume, A., and R. G. Griffin. 1982. Carbon-13 and deuterium nuclear magnetic resonance study of the interaction of cholesterol with phosphatidylethanolamine. *Biochemistry.* 21:6230–6242.

45. Gally, H. U., A. Seelig, and J. Seelig. 1976. Cholesterol-induced rod-like motion of fatty acyl chains in lipid bilayers a deuterium magnetic resonance study. *Hoppe Seylers Z. Physiol. Chem.* 357:1447–1450.

46. Haberkorn, R. A., R. G. Griffin, M. D. Meadows, and E. Oldfield. 1977. Deuterium nuclear magnetic resonance investigation of the dipalmitoyl lecithin-cholesterol-water system. *J. Am. Chem. Soc.* 99:7353–7355.

47. Oldfield, E., M. Meadows, D. Rice, and R. Jacobs. 1978. Spectroscopic studies of specifically deuterium labeled membrane systems. Nuclear magnetic resonance investigation of the effects of cholesterol in model systems. *Biochemistry.* 17:2727–2740.

48. Shepherd, J. C., and G. Buldt. 1978. Zwitterionic dipoles as a dielectric probe for investigating headgroup mobility in phospholipid membranes. *Biochim. Biophys. Acta.* 514:83–94.

49. Buldt, G., H. U. Gally, A. Seelig, J. Seelig, and G. Zaccai. 1978. Neutron diffraction studies on selectively deuterated phospholipid bilayers. *Nature.* 271:182–184.